

Spin gap in quasi-one-dimensional S=3/2 antiferromagnet $CoTi_2O_5$

Hao-Hang Xu(徐浩航), Qing-Yuan Liu(刘庆元), Chao Xin(辛潮), Qin-Xin Shen(申沁鑫), Jun Luo(罗军), Rui Zhou(周睿), Jin-Guang Cheng(程金光), Jian Liu(刘健), Ling Ling Tao(陶玲玲), Zhi-Guo Liu(刘志国), Ming-Xue Huo(霍明学), Xian-Jie Wang(王先杰), and Yu Sui(隋郁)
Citation: Chin. Phys. B, 2024, 33 (**3**): 037505. DOI: 10.1088/1674-1056/ad1381
Journal homepage: http://cpb.iphy.ac.cn; http://iopscience.iop.org/cpb

What follows is a list of articles you may be interested in

Creation and annihilation of artificial magnetic skyrmions with the electric field

Jun Cheng(程军), Liang Sun(孙亮), Yike Zhang(张一可), Tongzhou Ji(吉同舟), Rongxing Cao(曹荣幸), Bingfeng Miao(缪冰锋), Yonggang Zhao(赵永刚), and Haifeng Ding(丁海峰)
Chin. Phys. B, 2024, 33 (**3**): 037501. DOI: 10.1088/1674-1056/ad188f

Oscillation of Dzyaloshinskii-Moriya interaction driven by weak electric fields

Runze Chen(陈润泽), Anni Cao(曹安妮), Xinran Wang(王馨苒), Yang Liu(柳洋), Hongxin Yang(杨洪新), and Weisheng Zhao(赵巍胜)
Chin. Phys. B, 2024, 33 (**2**): 027501. DOI: 10.1088/1674-1056/ad0f85

Controllable high Curie temperature through 5d transition metal atom doping in CrI_3

Xuebing Peng(彭雪兵), Mingsu Si(司明苏), and Daqiang Gao(高大强)
Chin. Phys. B, 2024, 33 (**1**): 017503. DOI: 10.1088/1674-1056/ad053b

Tuning magneto-dielectric properties of Co_2Z ferrites via Gd doping for high-frequency applications

Jian Wu(武剑), Bing Lu(卢冰), Ying Zhang(张颖), Yixin Chen(陈一鑫), Kai Sun(孙凯), Daming Chen(陈大明), Qiang Li(李强), Yingli Liu(刘颖力), and Jie Li(李颉)
Chin. Phys. B, 2023, 32 (**9**): 097501. DOI: 10.1088/1674-1056/acc3f7

Electric-field control of perpendicular magnetic anisotropy by resistive switching via electrochemical metallization

Yuan Yuan(袁源), Lu-Jun Wei(魏陆军), Yu Lu(卢羽), Ruo-Bai Liu(刘若柏), Tian-Yu Liu(刘天宇), Jia-Rui Chen(陈家瑞), Biao You(游彪), Wei Zhang(张维), Di Wu(吴镝), and Jun Du(杜军)
Chin. Phys. B, 2023, 32 (**6**): 067505. DOI: 10.1088/1674-1056/acbde8

Spin gap in quasi-one-dimensional $S = 3/2$ antiferromagnet $CoTi_2O_5$

Hao-Hang Xu(徐浩航)[1], Qing-Yuan Liu(刘庆元)[1,5], Chao Xin(辛潮)[2], Qin-Xin Shen(申沁鑫)[3], Jun Luo(罗军)[3], Rui Zhou(周睿)[3], Jin-Guang Cheng(程金光)[3], Jian Liu(刘健)[4], Ling-Ling Tao(陶玲玲)[1], Zhi-Guo Liu(刘志国)[1], Ming-Xue Huo(霍明学)[4], Xian-Jie Wang(王先杰)[1], and Yu Sui(隋郁)[1,4,†]

[1] *School of Physics, Harbin Institute of Technology, Harbin* 150001, *China*
[2] *School of Science, Changchun University of Science and Technology, Changchun* 130022, *China*
[3] *Beijing National Laboratory for Condensed Matter Physics, and Institute of Physics, Chinese Academy of Sciences, Beijing* 100190, *China*
[4] *Laboratory for Space Environment and Physical Sciences, Harbin Institute of Technology, Harbin* 150001, *China*
[5] *Southwest Institute of Applied Magnetics, Mianyang* 621000, *China*

(Received 15 September 2023; revised manuscript received 26 November 2023; accepted manuscript online 8 December 2023)

Quasi-one-dimensional (1D) antiferromagnets are known to display intriguing phenomena especially when there is a spin gap in their spin-excitation spectra. Here we demonstrate that a spin gap exists in the quasi-1D Heisenberg antiferromagnet $CoTi_2O_5$ with highly ordered Co^{2+}/Ti^{4+} occupation, in which the Co^{2+} ions with $S = 3/2$ form a 1D spin chain along the a-axis. $CoTi_2O_5$ undergoes an antiferromagnetic transition at $T_N \sim 24$ K and exhibits obvious anisotropic magnetic susceptibility even in the paramagnetic region. Although a gapless magnetic ground state is usually expected in a quasi-1D Heisenberg antiferromagnet with half-integer spins, by analyzing the specific heat, the thermal conductivity, and the spin-lattice relaxation rate $(1/T_1)$ as a function of temperature, we found that a spin gap is opened in the spin-excitation spectrum of $CoTi_2O_5$ around T_N, manifested by the rapid decrease of magnetic specific heat to zero, the double-peak characteristic in thermal conductivity, and the exponential decay of $1/T_1$ below T_N. Both the magnetic measurements and the first-principles calculations results indicate that there is spin-orbit coupling in $CoTi_2O_5$, which induces the magnetic anisotropy in $CoTi_2O_5$, and then opens the spin gap at low temperature.

Keywords: quasi-one-dimensional antiferromagnet, magnetic anisotropy, spin gap

PACS: 75.50.Ee, 75.30.Gw **DOI:** 10.1088/1674-1056/ad1381

1. Introduction

Low-dimensional quantum magnets have been attracting much attention due to their fascinating phenomena, such as Bose–Einstein condensation, quantum spin liquids, and multiferroics.[1–3] Among various low-dimensional materials, the 1D magnets with a spin gap are of particular interest because they can host many exotic ground states, such as the field-induced gapless quantum spin liquid state in $BaCo_2V_2O_8$,[4] and the pressure-induced superconductivity in $Sr_2Ca_{12}Cu_{24}O_{41}$.[5] In general, for a uniform 1D Heisenberg antiferromagnetic spin chain, the value of the spin quantum number S determines the appearance of the spin gap in the excited states.[6] The spin gap can only be observed in 1D Heisenberg antiferromagnets with integer spins, e.g., $PbNi_2V_2O_8$ with $S = 1$, in which a Haldane gap exists in the magnetic excitation spectrum,[7] while a gapless magnetic ground state can be seen when S is half-integer. However, in some special cases, 1D antiferromagnets with half-integer spins also exhibit the gapped ground state by breaking the translation symmetry of spin.[8–10] For example, in the spin-Peierls compound $CuGeO_3$, the dimerization of Cu^{2+} with $S = 1/2$ not only leads to the structural transition but also opens a spin gap in the magnetic excitation spectrum.[11] In addition, the spin gap was also found in some 1D $S = 1/2$ antiferromagnets with special crystal and magnetic structures, such as Cu benzoate and $BaCo_2V_2O_8$.[12–14] For Cu benzoate with alternating crystal axes, it shows a field-induced spin gap because a non-collinear spin arrangement can be induced by applying a magnetic field perpendicular to the spin chain, and the canted spins are stabilized by the internal effective field along the chain.[15] However, in the case of $BaCo_2V_2O_8$, the non-collinear magnetic structure is generated by the screw chain of Co^{2+} and stabilized by the interchain exchange interaction. Thus, the spin gap in $BaCo_2V_2O_8$ opens with the 3D long-range magnetic ordering under zero field and can be closed under the magnetic field of about 40 kOe, followed by the field-induced order-to-disorder phase transition.[13,16]

The spin chain of Co^{2+} could also exist in the pseudobrookite $CoTi_2O_5$, which belongs to the orthorhombic crystal system with a *Cmcm* space group. The $CoTi_2O_5$ consists of two inequivalent $TM1O_6$ and $TM2O_6$ octahedrons with a ratio of 1:2, where TM represents Co^{2+}/Ti^{4+} cations. In comparison to the $TM2O_6$ octahedron, the $TM1O_6$ octahedron in pseudobrookite compounds is larger and more distorted. Therefore, the cation order-disorder always occurs in pseudobrookite compounds. For the completely ordered

†Corresponding author. E-mail: suiyu@hit.edu.cn
© 2024 Chinese Physical Society and IOP Publishing Ltd

$CoTi_2O_5$, as shown in Fig. 1(a), the larger $TM1O_6$ octahedron can only be occupied by the Co^{2+} ($r = 0.74$ Å), and the nonmagnetic Ti^{4+} ($r = 0.68$ Å) occupies the $TM2O_6$ octahedron, just like the well-studied pseudobrookite $MgTi_2O_5$.[17] In this situation, the distances between different Co^{2+} along the b and c directions are much greater than that along the a-axis ($a = 3.72649$ Å, $b = 9.7005$ Å, $c = 10.0731$ Å),[18] so a 1D chain of Co^{2+} could form along the a-axis, making $CoTi_2O_5$ an example of a quasi-1D antiferromagnet with spin $S = 3/2$.

Recently, Kirschner *et al.* reported that $CoTi_2O_5$ shows an unexpected long-range antiferromagnetic ordering at $T_N = 26$ K, though there is a strong frustration of Co^{2+} according to the magnetic structure of $CoTi_2O_5$.[18] They proposed that there could be the spin Jahn–Teller effect in $CoTi_2O_5$, which lowers the structural symmetry and relieves the frustration, and in turn, leads to the appearance of the magnetic transition. However, the nature of $CoTi_2O_5$ as a 1D antiferromagnet has yet to be reported and whether a spin gap exists in $CoTi_2O_5$ is still unknown. In this work, we grew the $CoTi_2O_5$ single crystals with highly ordered Co^{2+}/Ti^{4+} occupation by using the floating zone method and revealed that $CoTi_2O_5$ is a quasi-1D Heisenberg antiferromagnet. The appearance of the spin-orbit coupling in $CoTi_2O_5$ causes the obvious magnetic anisotropy, which opens a spin gap at low temperature.

2. Experiments

2.1. Single-crystal growth and characterization

$CoTi_2O_5$ single crystals were prepared by the optical floating zone technique in an image furnace with two ellipsoidal mirrors (IR Image Furnace G3, Quantum Design Japan).[18,19] The crystals were grown in different atmospheres (pure Ar, pure O_2, and Ar/O_2 mixed gas atmosphere) with a growth rate varying from 1 to 10 mm/h. $CoTi_2O_5$ single crystal with highly ordered Co^{2+}/Ti^{4+} occupation was grown under pure Ar atmosphere with the growth rate of 1 mm/h. This gives a new approach for manipulating the ordering of cations and producing 1D spin chains. $MgTi_2O_5$ single crystals were also prepared under the pure argon atmosphere with 1 mm/h to estimate the lattice specific heat of $CoTi_2O_5$. The phase purity was identified by the x-ray diffraction (XRD, Aeris, Cu K_{α_1} radiation) and the x-ray Laue back diffraction was used to determine the crystal principal axes. Raman spectra were obtained with the LabRAM HR Evolution Raman Spectrometer (HORIBA). X-ray photoelectron spectroscopy (XPS) was measured with Esca Xi+ (ThermoFisher).

2.2. Magnetization and thermal properties measurements

The temperature and magnetic-field dependencies of magnetization $M(T)$ and $M(H)$ were recorded using a commercial SQUID magnetometer (MPMS3) up to the field of 70 kOe. The measurement of specific heat $C(T)$ was performed with a physical property measurement system (PPMS, DynaCool-14 T). Both the thermal expansion $\Delta L/L_0(T)$ and the magnetostriction $\Delta L/L_0(H)$ were performed in the PPMS by using an AH 2550A capacitance dilatometer that was calibrated with 99.999% pure Cu and Al rods. The thermal conductivity $\kappa(T)$ was measured in the PPMS with the method of one heater and two thermometers.

2.3. NMR measurements

In experiment, ^{59}Co NMR measurements were performed on a single crystal of $CoTi_2O_5$ under a fixed magnetic field $H = 90.743$ kOe. The NMR spectra were obtained by integrating the spin echo as a function of frequency. The spin-lattice relaxation rate $1/T_1$ was measured by the saturation-recovery method. The ^{59}Co T_1 was obtained by fitting the nuclear magnetization $M(t)$ with the equation $1 - M(t)/M(0) = 0.01191\exp(-t/T_1) + 0.06818\exp(-6t/T_1) + 0.20604\exp(-15t/T_1) + 0.71387\exp(-28t/T_1)$, where $M(0)$ and $M(t)$ are the nuclear magnetizations at the thermal equilibrium and at time t, respectively, after the comb pulse.

2.4. Theoretical calculations

All of our first-principles calculations were based on spin-polarized density functional theory (DFT) as implemented in the Vienna *ab initio* simulation package (VASP).[20,21] The Perdew–Burke–Ernzerhof functional revised for solids (PBEsol) was adopted for exchange–correlation potential. Generalized gradient approximation (GGA)[22] with the Hubbard parameter (GGA+U)[23] was employed to solve the Kohn–Sham equation.[24] The plane wave energy cutoff, convergence in energy, and residual force on each atom were set to 500 eV, 1×10^{-5} eV, and 0.01 eV/Å, respectively. To obtain the accurate magnetic structure, we built a $2 \times 1 \times 1$ supercell, and the corresponding Brillouin zone integrations were set using a tetrahedron method in $8 \times 8 \times 8$ Monkhorst–Pack K-point mesh.[25] Magnetic anisotropy and spin–orbital coupling (SOC) were considered. The structure and spin density visualization and analysis were carried out using the VESTA code.[26]

3. Results and discussions

3.1. Controlling the degree of the ordering of Co^{2+}/Ti^{4+} in $CoTi_2O_5$

It was reported that the highly ordered cation occupation in the pseudobrookite ceramics can be obtained by using the high-pressure technique or by annealing the sample at a lower temperature.[17,27] In our previous work, we found that the single crystal of inverse spinel Mn_2TiO_4 with ordered Mn^{2+}/Ti^{4+} occupation at B sites can be grown by the optical floating zone method under pure Ar atmosphere.[28] Thus, we prepared the $CoTi_2O_5$ single crystals with different degrees of Co^{2+}/Ti^{4+} ordering by using the floating zone technique under pure Ar, pure O_2, and the Ar/O_2 mixed gas atmosphere.

The clear Laue diffraction spots show the high quality of our single crystal, as illustrated in Fig. 1(c). The XPS spectra of Co-2p and Ti-2p show that the oxidation states of Co and Ti in the grown $CoTi_2O_5$ sample are +2 and +4, respectively (details can be seen in Fig. S1 in the supplemental material). The $M(T)$ curves of crystals grown with different conditions were recorded to roughly check the degree of the ordering of Co^{2+}/Ti^{4+} because the character of the 1D magnets, usually represented by the broad peak at high temperature in the $M(T)$ curves, depends on the degree of the ordering of Co^{2+}/Ti^{4+} in $CoTi_2O_5$. As shown in Fig. 1(b), the broad peak in $M(T)$ becomes more pronounced with decreasing oxygen content in the growth atmosphere, suggesting that Co^{2+}/Ti^{4+} tends to be ordered in the pure Ar atmosphere. Furthermore, when the growth rate is lowered, the magnetization below the magnetic ordering temperature decreases more rapidly, and the Curie tail gradually becomes weaker, revealing that the Co^{2+}/Ti^{4+} occupation becomes more ordered.

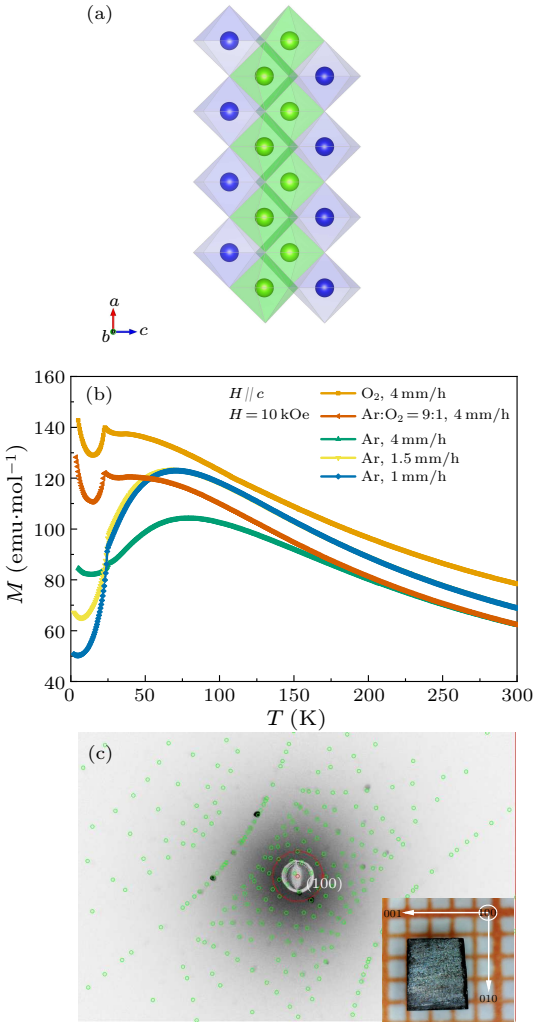


Fig. 1. (a) Crystal structure of $CoTi_2O_5$. Co^{2+} and Ti^{4+} are labeled as blue and green balls, respectively. (b) The $M(T)$ curves of $CoTi_2O_5$ single crystals prepared under different conditions. (c) Laue pattern taken from the $CoTi_2O_5$ single crystal along the [100] direction. Inset in (c) shows the oriented single crystal with three axes [100], [010], and [001].

3.2. Determining the degree of the ordering of Co^{2+}/Ti^{4+} in $CoTi_2O_5$

Raman spectra of $CoTi_2O_5$ grown under different conditions were measured to estimate the degree of the ordering of Co^{2+}/Ti^{4+}. As shown by the asterisks in Fig. 2(a), extra vibrate modes appear in the crystals prepared under the pure Ar atmosphere, consistent with the results of the well-studied $MgTi_2O_5$ with highly ordered Mg^{2+}/Ti^{4+} occupation.[29] It was reported in $MgTi_2O_5$ that the frequency ω of the $B_{1g}(5)$ Raman mode at 640(2) cm^{-1} shows the blue shift with the Mg^{2+}/Ti^{4+} disorder increasing and can be used to determine the Mg^{2+}/Ti^{4+} disorder parameter X with the relation[29]

$$\omega = 629(1)\ \mathrm{cm}^{-1} + 60(5)X\ \mathrm{cm}^{-1}, \tag{1}$$

where X is defined as the atomic concentration of Ti^{4+} in TM1 sites. The Raman spectra of $CoTi_2O_5$ also show a similar blue shift, so the Co^{2+}/Ti^{4+} disorder parameter X for the most ordered $CoTi_2O_5$ is estimated to be in the range of [0.12, 0.18] by using formula (1), which is comparable with [0.15, 0.22] of highly ordered $MgTi_2O_5$ prepared by annealing.[29,30] (the blue shift in Raman spectra of $CoTi_2O_5$ can be seen in Fig. S2 in the supplemental material).

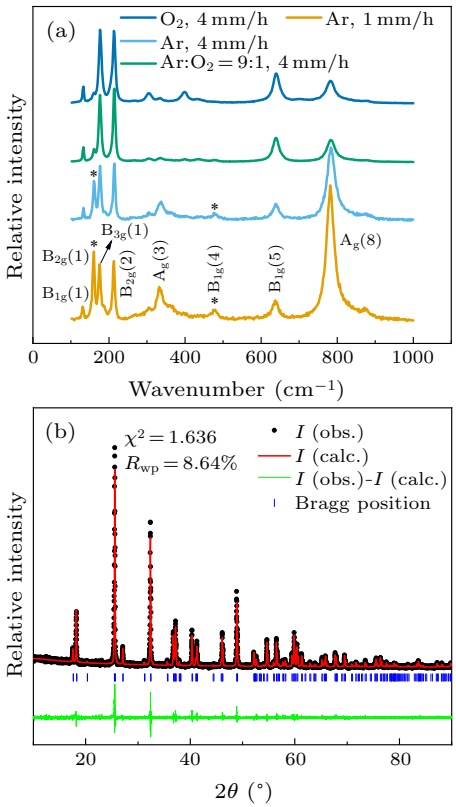


Fig. 2. (a) The Raman spectra of $CoTi_2O_5$ single crystals prepared under different conditions. (b) The Rietveld refinement results of $CoTi_2O_5$ prepared under pure Ar atmosphere with 1 mm/h.

From the powder XRD data of the most ordered $CoTi_2O_5$ crystal, as shown in Fig. 2(b), the lattice parameters of $CoTi_2O_5$ are refined as $a = 3.72284(2)$ Å, $b = 9.70068(5)$ Å,

and $c = 10.06784(5)$ Å, consistent with the results from neutron powder diffraction reported before.[18] The refinement results further give the Co^{2+}/Ti^{4+} disorder parameter X about 0.13, showing that most of the Co^{2+} occupy the TM1 sites, forming the Co^{2+} chain along the a-axis. Thus, the $CoTi_2O_5$ single crystal with highly ordered Co^{2+}/Ti^{4+} occupation can be grown in the pure Ar atmosphere at a growth rate of 1 mm/h. This provides a new way for controlling the ordering of cations and then generating 1D spin chains. The magnetization, the thermal physical properties, and the ^{59}Co nuclear magnetic resonance spectra measurements are all performed on the oriented $CoTi_2O_5$ single crystals with the highest degree of the ordering of Co^{2+}/Ti^{4+}, which was grown in the pure Ar atmosphere at a growth rate of 1 mm/h (refined crystal structure parameters of $CoTi_2O_5$ can be seen in Table S1 in the supplemental material).

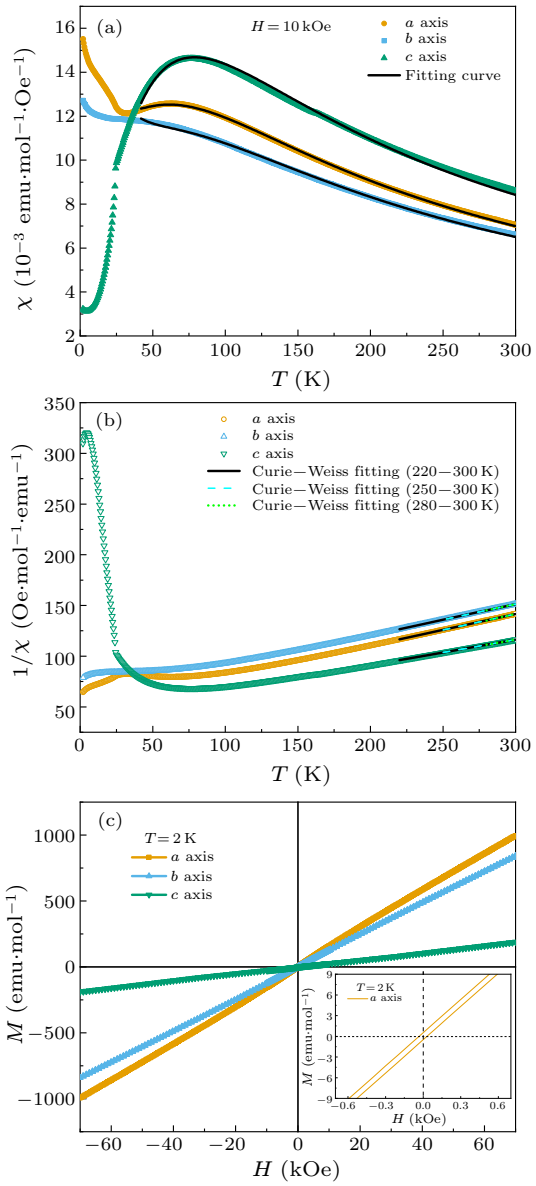


Fig. 3. The magnetic measurements of the oriented $CoTi_2O_5$ single crystals: (a) $\chi(T)$, (b) $1/\chi$, (c) $M(H)$. Inset in (c) shows the enlarged hysteresis part in the a-axis.

3.3. Magnetization measurements

In Fig. 3(a), the $\chi(T)$ curve of the $CoTi_2O_5$ crystal along three major crystallographic axes shows a broad peak at about 80 K, which is a typical sign of the 1D short-range magnetic ordering. A sharp decrease at $T_N \sim 24$ K in the $\chi(T)$ along the c-axis of $CoTi_2O_5$ corresponds to the long-range antiferromagnetic ordering of Co^{2+}. Conversely, below T_N, the magnetic susceptibilities along the a and b axes increase with decreasing temperature. This apparent anisotropic behavior of the $\chi(T)$ curves illustrates that the c-axis is the easy axis in $CoTi_2O_5$ while the spin chain of Co^{2+} forms along the a-axis, in accordance with the magnetic structure obtained from the neutron diffraction spectra.[18] The $\chi(T)$ curve above 40 K can be well fitted by using the Pade approximation for the Heisenberg spin chain model,[31] as shown in Fig. 3(a), indicating that Co^{2+} forms the uniform 1D $S = 3/2$ chain in $CoTi_2O_5$. The fitting result gives the value of g-factor in $CoTi_2O_5$ along different axes as $g_a \sim 2.45$, $g_b \sim 2.39$, and $g_c \sim 2.67$, explaining the difference of the susceptibilities at 300 K. Due to the maximum of the broad peak in $\chi(T)$ locates at about 80 K, the $1/\chi$–T curve of $CoTi_2O_5$ was fitted in multiple intervals above 220 K with the Curie–Weiss law to avoid the influence of short-range magnetic correlation, as shown in Fig. 3(b). The obtained effective magnetic moments along the a, b, and c axes are 5.0(1) μ_B, 5.1(1) μ_B, and 5.6(1) μ_B, respectively, which are much larger than the spin-only value of 3.87 μ_B for the Co^{2+} with $S = 3/2$, indicating that there is a large orbital contribution to the magnetic moment in $CoTi_2O_5$. From the $M(H)$ loops at 2 K of all the three axes in Fig. 3(c), an obvious magnetic anisotropy can be seen, and the three axes all show an apparent hysteresis behavior with coercive filed around 100 Oe. Both the behaviors of $M(T)$ and $M(H)$ suggest the appearance of spin-orbit coupling (SOC) in $CoTi_2O_5$, which could induce the single-ion anisotropy or the Dzyaloshinskii–Moriya interaction.

However, though the SOC is usually considered to be negligible for systems with 3d transition-metal ions,[32] it can be seen in some materials containing Co^{2+} with a highspin state, e.g., $CoNb_2O_6$.[33] The appearance of SOC combined with the octahedral crystal field normally causes Co^{2+} to show an effective spin $S = 1/2$.[34] To further confirm the existence of the SOC in $CoTi_2O_5$, the first-principles calculations were performed. To explain the behavior of spin polarization for $CoTi_2O_5$ in the *Cmcm* phase, the total and partial density of states (DOS) of Ti, Co-3d, and O-2p, are shown in Fig. 4. The total DOSs of spin-up and spin-down electrons are similar to each other and conform to the desired antiferromagnetic state. The band gap estimated from Fig. 4(a) is about ~ 2.02 eV. The energy region near the Fermi level is mainly composed by the 3d states of Co^{2+} and O-2p states. The energy positions of the O-2p states overlap with those of the Co-3d and Ti-3d states,

indicating the hybridization between O-2p and Co, Ti-3d orbitals. The number of unpaired electrons of Co^{2+} is calculated to be 2.72, consistent with the results obtained from the neutron powder diffraction experiments.[18] From the partial DOS of the Co atom in Fig. 4(c), the Co^{2+} is in the high spin state $3d^7(t_{2g}^5 e_g^2)$ with $S = 3/2$.

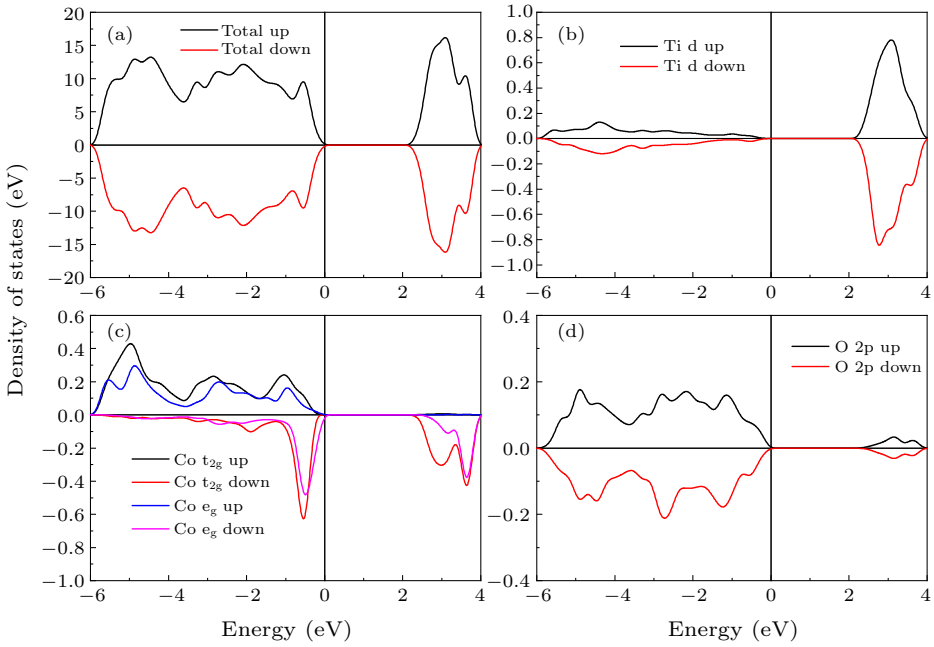


Fig. 4. Total and partial density of states for $CoTi_2O_5$ within the *Cmcm* symmetry calculated by GGA+U. (a) The total DOS of $CoTi_2O_5$. (b) Partial DOS of d character for Ti. (c) Partial DOS of t_{2g} and e_g characters for Co. (d) Partial DOS of 2p character for O.

According to the magnetic propagation vector $\boldsymbol{k} = (1/2, 1/2, 0)$ in $CoTi_2O_5$ reported in Ref. [18], we build a $2 \times 2 \times 1$ supercell to satisfy the antiferromagnetic structure and consider the SOC to compute the magnetic anisotropy energy (details are given in the supplemental material). The calculation results suggest that, when considering SOC, the total energy of $CoTi_2O_5$ is about -478.806 eV, which is obviously lower than the -478.540 eV without SOC, confirming the existence of the SOC in $CoTi_2O_5$. Since the CoO_6 octahedron in $CoTi_2O_5$ is highly distorted, we think that the distorted crystal field of $CoTi_2O_5$ prevents SOC to reduce the effective spin of Co^{2+} to 1/2, resulting in Co^{2+} with a high-spin state remaining $S = 3/2$ in $CoTi_2O_5$.

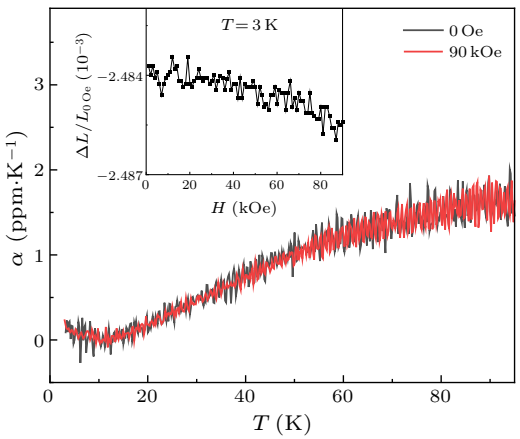


Fig. 5. The thermal expansion coefficient of $CoTi_2O_5$ single crystal. Inset shows the magnetostriction effect of $CoTi_2O_5$ single crystal at $T = 3$ K.

3.4. Thermal physical properties measurements

The behavior of the phase transition of $CoTi_2O_5$ was characterized by using specific heat measurements. There is only one λ shaped peak at antiferromagnetic ordering temperature $T_N = 24$ K in the specific heat curve of $CoTi_2O_5$, as shown by the black line in Fig. 6(a). Kirschner *et al.* proposed that a spin Jahn–Teller effect occurs at T_N, but no experimental evidence was given for any structural distortion.[18] We measured the thermal expansion and magnetostriction of $CoTi_2O_5$ single crystal, as shown in Fig. 5, and found that neither the anomaly of the thermal expansion coefficient around T_N nor the magnetostriction phenomenon below T_N can be seen, indicating that there is no strong spin–lattice coupling in $CoTi_2O_5$. Therefore, it is reasonable to believe that the λ-shaped peak in $C(T)$ only comes from the antiferromagnetic ordering of $CoTi_2O_5$. In the critical region around T_N, the $C(T)$ curve can be fitted with the following function:[35]

$$C(T) = B^{\pm} + F^{\pm}t + A^{\pm}|t|^{-\alpha}(1 + E^{\pm}|t|^{0.5}), \qquad (2)$$

where $t = (T - T_N)/T_N$ represents the reduced temperature, α is the critical exponent, and $A^{\pm}$, $B^{\pm}$, $F^{\pm}$, and $E^{\pm}$ are adjustable parameters. Superscripts $+$ and $-$ represent $T > T_N$ and $T < T_N$, respectively. Within the range of $10^{-3} < |t| < 10^{-1}$ in the vicinity of T_N, the experimental data can be perfectly fitted with Eq. (2), as shown in Fig. 6(b). The obtained fitting parameters and critical exponents are listed in Table 1. The values of the critical exponent is obtained to be $\alpha^+ = -0.16$ and

$\alpha^- = -0.12$, far away from $\alpha = 0.11$ for the Ising model or the $\alpha = -0.01$ for the XY model, whereas close to $\alpha = -0.12$ for the Heisenberg model.[36] Although a gapless magnetic ground state is usually expected in a quasi-1D Heisenberg antiferromagnet with half-integer spins, according to the theory of spin waves,[37] the uniaxial magnetic anisotropy in $CoTi_2O_5$ can open a spin gap in its magnetic excitation spectrum.

The magnetic specific heat $C_m(T)$ of $CoTi_2O_5$ was obtained by subtracting the lattice specific heat $C_p(T)$ from the total specific heat of $CoTi_2O_5$, as shown in Fig. 6(c). With the decreasing temperature below T_N, the $C_m(T)$ of $CoTi_2O_5$ decreases quickly and tends to zero at low temperature, implying that a spin gap appears in $CoTi_2O_5$. The C_p of the $CoTi_2O_5$ single crystal was estimated from the C_p of the $MgTi_2O_5$ single crystal by using the formula $C_p(T)_{CoTi_2O_5} = \sqrt{M_{CoTi_2O_5}/M_{MgTi_2O_5}}C_p(T)_{MgTi_2O_5}$, in which $M_{CoTi_2O_5}$ and $M_{MgTi_2O_5}$ represent the relative molecular masses of $CoTi_2O_5$ and $MgTi_2O_5$, respectively. The magnetic entropy change of $CoTi_2O_5$ calculated from $\Delta S = \int_{T_1}^{T_2} \frac{C_m}{T} dT$ is much smaller than $R\ln 4 \approx 11.52$ J·mol^{-1}·K^{-1} at T_N (R is the gas constant), indicating that the magnetic entropy is released far above T_N by the short-range magnetic ordering due to the formation of the 1D Co^{2+} spin chain in $CoTi_2O_5$.

Table 1. Adjustable fitting parameters, and critical parameters of the fittings of the specific heat for $CoTi_2O_5$.

	A	B	F	E	α	Fitted T_N (K)	Measured T_N (K)
$T < T_N$	−20.79	23.95	5.22×10^{-6}	0.44	−0.12	24.41	24
$T > T_N$	−51.85	28.41	−146.40	−2.64	−0.16	24.18	

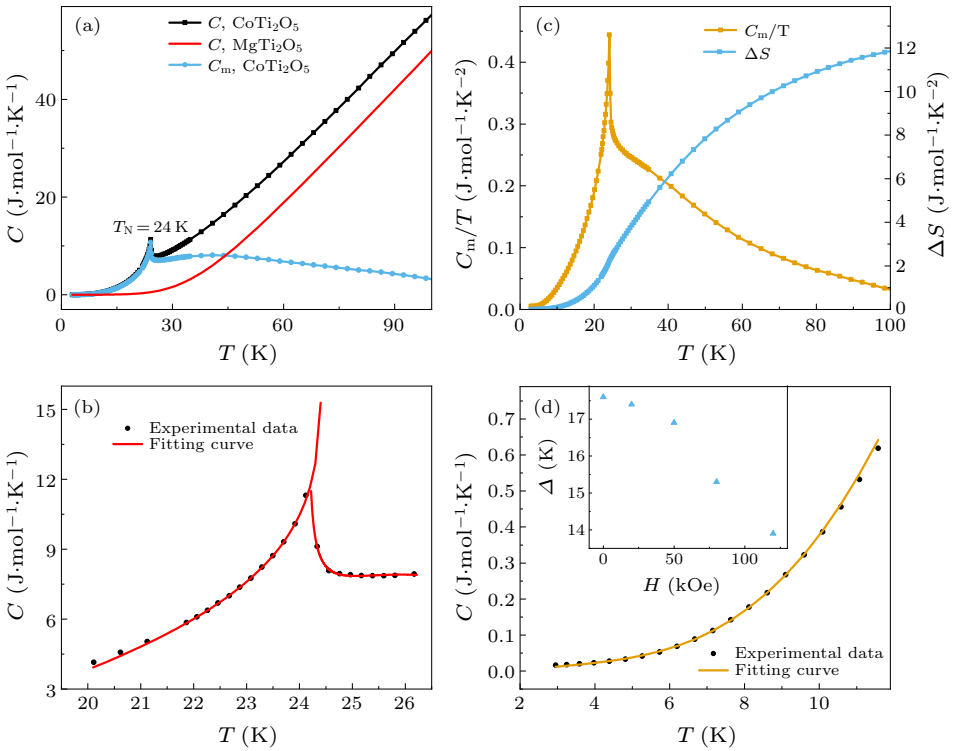


Fig. 6. The experimental and fitted specific heat curves of $CoTi_2O_5$ single crystal under zero magnetic field. (a) The specific heat of $CoTi_2O_5$ and $MgTi_2O_5$. The latter is used to subtract the lattice specific heat. (b) The critical behavior fitted from Eq. (2). (c) The magnetic specific heat and change of entropy of $CoTi_2O_5$. (d) The low-temperature specific heat data fitted with Eq. (3). The inset shows the magnetic field dependency of Δ, which was also fitted with Eq. (3).

To determine the presence of the spin gap, the specific heat data of $CoTi_2O_5$ at the low temperature was fitted with Eq. (3), which is extensively used in 1D antiferromagnets, like $CuGeO_3$ and NaV_2O_5,[38,39] to roughly estimate the value of the spin gap:

$$C(T) = GT^3 + Qe^{-\Delta/T}, \tag{3}$$

where G and Q stand for the coefficients, and Δ represents the value of the spin gap. The fitting result agrees well with the experimental data, as shown in Fig. 6(d), and the Δ is obtained to be about 17.6 K. The low-temperature specific heat data under different magnetic fields was also fitted with Eq. (3), as shown by the inset in Fig. 6(d), illustrating that the value of the spin gap decreases with the increase of the magnetic field. This means that the spin gap in $CoTi_2O_5$ can be suppressed by the magnetic field.

As a sensitive probe for the scattering of phonon and magnon,[40] the thermal conductivity of the $CoTi_2O_5$ crystal

was also measured to investigate the behavior of the spin gap in $CoTi_2O_5$. In Fig. 7(a), the $\kappa(T)$ curve of the $CoTi_2O_5$ single crystal shows two obvious peaks at about 80 K and $T^* \sim 12$ K when applying the heat flow along the chain direction (a-axis). To figure out the origin of these two peaks, the phonon thermal conductivity (κ_{ph}) was fitted with the Debye model as follows:[41]

$$\kappa_{ph}(T) = \frac{3dNRT^3v^2}{M\Theta_D^3}\int_0^{\Theta_D/T}\frac{x^4 e^x}{(e^x-1)^2}\tau(T,x)\,dx, \quad (4)$$

where d, N, R, M, and $x = \frac{\hbar\omega}{k_B T}$ represent the mass density, the number of atoms composing $CoTi_2O_5$, the gas constant, the molar weight, and the reduced phonon frequency, respectively. Debye temperature $\Theta_D = 673.3$ K of $CoTi_2O_5$ is obtained from the specific heat measurement. The mean sound velocity $v = 7120$ m/s of $CoTi_2O_5$ is calculated from Θ_D by using the equation $v = \Theta_D(k_B/\hbar)(6\pi^2 n)^{-1/3}$, in which n is the atomic number density. The scattering mechanisms of phonon in $CoTi_2O_5$ consist of the boundary phonon scattering $\tau_b^{-1} = v/L$, the scattering by point defects $\tau_{pd}^{-1} = p(Tx)^4$, and the phonon umklapp processes $\tau_{um}^{-1} = UxT\exp(-\frac{\Theta_D}{bT})$, where p, U, and b are adjustable parameters, and L represents the length of the sample. Thus, the total relaxation time τ can be calculated as $\tau^{-1} = \tau_b^{-1} + \tau_{pd}^{-1} + \tau_{um}^{-1}$. The fitting curve matches well with the experimental data below T_N, as shown by the dashed line in Fig. 7(a), and the parameters are achieved as $p = 3.9\times10^3$ K^{-4}·s^{-1}, $U = 2.3\times10^7$ s^{-1}, $b = 16$, which are reasonable for an insulator,[42,43] demonstrating that the low-temperature peak at T^* in $\kappa(T)$ is the phonon peak and the high-temperature peak in $\kappa(T)$ comes from the contribution of magnon. This double-peak behavior was also found in the $\kappa(T)$ curve along the spin chain direction in some quasi-1D antiferromagnets, such as $Sr_{14}Cu_{24}O_{41}$,[44] because the magnetic excitations propagate along the spin chain direction. The magnon thermal conductivity κ_m of $CoTi_2O_5$ can be obtained by deducting the κ_{ph} from the total thermal conductivity of $CoTi_2O_5$, as shown by the solid line in Fig. 7(a). As the temperature decreases, κ_m of $CoTi_2O_5$ reaches a maximum at ~ 80 K, illustrating that the high-temperature magnon peak is caused by the boundary scattering of the magnon. More importantly, κ_m vanishes around T_N, meaning that the spin gap occurs together with the antiferromagnetic ordering in $CoTi_2O_5$ because the heat transport from magnon is interrupted by the opening of the spin gap in $CoTi_2O_5$.

When applying a magnetic field of 90 kOe, the peak at T^* in $\kappa(T)$ is significantly suppressed, as shown in Fig. 7(b), while the magnon peak around 80 K is almost field-independent because the short-range magnetic ordering of Co^{2+} cannot be destroyed by the magnetic field. Since the phonon thermal conductivity should be independent of the magnetic field, the weakness of $\kappa(T)$ below T_N under 90 kOe shows that the spin gap tends to be closed by the magnetic field, and then the reappearance of the phonon-magnon scattering results in the suppression of the phonon peak in $\kappa(T)$ under the strong field. Assuming that phonons at low temperature are scattered only by magnons on the triplet after applying the magnetic field, then the magnetic field dependence of κ_{ph} can be given by Eq. (5), which was successfully used to describe the thermal transport behavior in some quasi-1D antiferromagnets under the low magnetic field, like $TlCuCl_3$ and $Pb_2V_3O_9$:[45,46]

$$\kappa(H) = \frac{1}{a + be^{-\Delta(H)/T}}, \quad (5)$$

where a and b are parameters and $\Delta(H)$ shows the field dependence of the spin gap. In this case, the spin gap usually changes linearly with the magnetic field and can be written as $\Delta(H) = \Delta(0) + wH$, in which $\Delta(0)$ is the value of the spin gap at zero fields and w is a coefficient.[47] The fitting curve overlaps with the experimental data well in low magnetic fields below 40 kOe, as shown by the inset in Fig. 7(b), and the $\Delta(0)$ is obtained to be about 14.0 K, close to the value of 17.6 K obtained from the specific heat data. The behavior of $\kappa(H)$ illustrates that the enhancement of the phonon-magnon scattering process with increasing magnetic field causes the decrease of κ, proving that the spin gap becomes smaller under the magnetic field. This is consistent with the fitting results of the specific heat shown in the inset of Fig. 6(d).

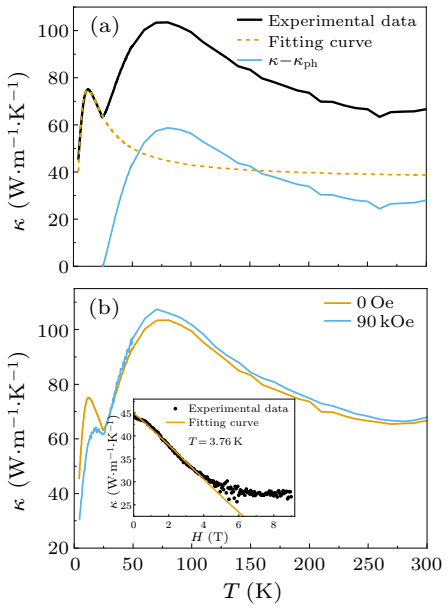


Fig. 7. The temperature-dependent thermal conductivity of $CoTi_2O_5$ single crystal along the a-axis: (a) $\kappa(T)$ at zero field, (b) $\kappa(T)$ at different fields. The inset in (b) shows the field-dependent thermal conductivity at the lowest temperature.

3.5. NMR measurements

To further confirm the existence of a spin gap in $CoTi_2O_5$, the ^{59}Co nuclear magnetic resonance (NMR) was measured to obtain the spin-lattice relaxation rate $1/T_1$, which is sensitive

to low-energy magnetic excitations and thus gives direct information on the presence of a spin gap (the measured ^{59}Co NMR spectra can be seen in the supplemental material). As shown in Fig. 8, the temperature dependence of $1/T_1$ is sharply suppressed with decreasing temperature below T_N and shows the activation behavior. By simply fitting with the relationship $1/T_1 \propto \exp(-\Delta/T)$, as shown in Fig. 8(b), the gap value of $\Delta \sim 35$ K was obtained, which is the same magnitude as the value roughly estimated from the specific heat data. The exponential decay of $1/T_1$ indicates the opening of a gap in the spin-excitation spectrum of $CoTi_2O_5$.

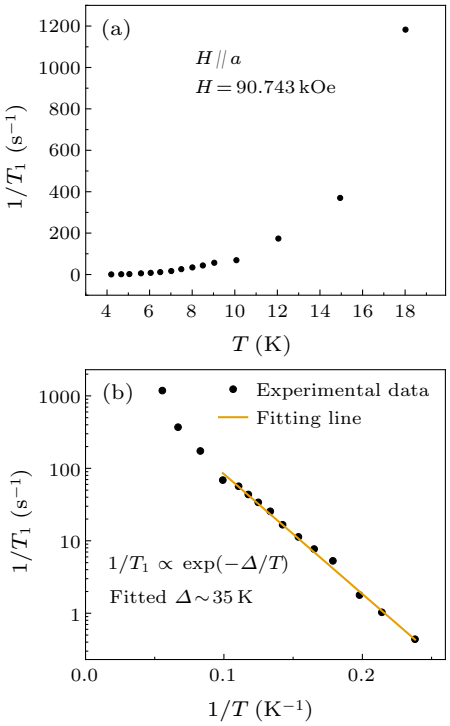


Fig. 8. The ^{59}Co spin-lattice relaxation rate $1/T_1$ measured for $H//a$-axis in $CoTi_2O_5$: (a) the temperature dependence of $1/T_1$, (b) the inverted-temperature dependence of $1/T_1$ below T_N.

4. Conclusion

The pseudobrookite $CoTi_2O_5$ single crystal with highly ordered Co^{2+}/Ti^{4+} occupation was grown under the pure Ar atmosphere, in which the Co^{2+} forms the uniform 1D spin chain with $S = 3/2$ and shows a long-range antiferromagnetic ordering at $T_N = 24$ K. Both the weak hysteresis behavior in $M(H)$ and first-principles calculations results confirm that there is the SOC in $CoTi_2O_5$, which leads to the apparent magnetic anisotropy. A spin gap appears around T_N, causing the evanishment of κ_m, the fast decrease of C_m, and the activation behavior of $1/T_1$ at low temperature. Additionally, the magnetic field can suppress the spin gap and thus enhance the phonon-magnon scattering, and finally results in the weakening of the phonon peak at T^* in $\kappa(T)$.

Acknowledgments

This work was supported by the National Natural Science Foundation of China (Grant No. 52372003) and the Funds from Beijing National Laboratory for Condensed Matter Physics. A portion of this work was carried out at the Synergetic Extreme Condition User Facility (SECUF).

References

[1] Zapf V, Jaime M and Batista C D 2014 *Rev. Mod. Phys.* **86** 563
[2] Clark L and Abdeldaim A H 2021 *Annu. Rev. Mater. Res.* **51** 495
[3] Hu T and Kan E 2019 *WIREs Comput. Mol. Sci.* **9** e1409
[4] Wang Z, Schmidt M, Loidl A, Wu J, Zou H, Yang W, Dong C, Kohama Y, Kindo K, Gorbunov D I, Niesen S, Breunig O, Engelmayer J and Lorenz T 2019 *Phys. Rev. Lett.* **123** 067202
[5] Fujiwara N, Môri N, Uwatoko Y, Matsumoto T, Motoyama N and Uchida S 2003 *Phys. Rev. Lett.* **90** 137001
[6] Oshikawa M, Yamanaka M and Affleck I 1997 *Phys. Rev. Lett.* **78** 1984
[7] Uchiyama Y, Sasago Y, Tsukada I, Uchinokura K, Zheludev A, Hayashi T, Miura N and Böni P 1999 *Phys. Rev. Lett.* **83** 632
[8] Paul S and Ghosh A K 2014 *J. Magn. Magn. Mater.* **362** 193
[9] Vasil'ev A N, Markina M M and Popova E A 2005 *Low Temp. Phys.* **31** 203
[10] Vasiliev A, Volkova O, Zvereva E and Markina M 2018 *npj Quantum Mater.* **3** 18
[11] Pouget J P, Regnault L P, Ain M, Hennion B, Renard J P, Veillet P, Dhalenne G and Revcolevschi A 1994 *Phys. Rev. Lett.* **72** 4037
[12] Dender D C, Hammar P R, Reich D H, Broholm C and Aeppli G 1997 *Phys. Rev. Lett.* **79** 1750
[13] Grenier B, Petit S, Simonet V, Canévet E, Regnault L-P, Raymond S, Canals B, Berthier C and Lejay P 2015 *Phys. Rev. Lett.* **114** 017201
[14] Pan B Y, Xu Y, Ni J M, Zhou S Y, Hong X C, Qiu X and Li S Y 2022 *Phys. Rev. Lett.* **129** 167201
[15] Liu J, Kittaka S, Johnson R D, Lancaster T, Singleton J, Sakakibara T, Kohama Y, van Tol J, Ardavan A, Williams B H, Blundell S J, Manson Z E, Manson J L and Goddard P A 2019 *Phys. Rev. Lett.* **122** 057207
[16] Kimura S, Yashiro H, Okunishi K, Hagiwara M, He Z, Kindo K, Taniyama T and Itoh M 2007 *Phys. Rev. Lett.* **99** 087602
[17] Suzuki Y and Shinoda Y 2011 *Sci. Technol. Adv. Mater.* **12** 034301
[18] Kirschner F K K, Johnson R D, Lang F, Khalyavin D D, Manuel P, Lancaster T, Prabhakaran D and Blundell S J 2019 *Phys. Rev. B* **99** 064403
[19] Balbashov A M, Mukhin A A, Ivanov V Y, Iskhakova L D and Voronchikhina M E 2017 *Low Temp. Phys.* **43** 965
[20] Kresse G and Furthmüller J 1996 *Phys. Rev. B* **54** 11169
[21] Kresse G and Joubert D 1999 *Phys. Rev. B* **59** 1758
[22] Blöchl P E 1994 *Phys. Rev. B* **50** 17953
[23] Dudarev S L, Botton G A, Savrasov S Y, Humphreys C J and Sutton A P 1998 *Phys. Rev. B* **57** 1505
[24] Kohn W and Sham L J 1965 *Phys. Rev.* **140** A1133
[25] Monkhorst H J and Pack J D 1976 *Phys. Rev. B* **13** 5188
[26] Momma K and Izumi F 2011 *J. Appl. Crystallogr.* **44** 1272
[27] Xirouchakis D, Smirnov A, Woody K, Lindsley D H and Andersen D J 2002 *Am. Mineral.* **87** 658
[28] Liu Q Y, Xu H H, Liu J, Liu Z G, Huo M X, Wang X J and Sui Y 2022 *J. Magn. Magn. Mater.* **546** 168864
[29] He M, Winkler B, Bauer J D, Bayarjargal L, Ruiz-Fuertes J, Alencar I, Morgenroth W, Refson K and Milman V 2017 *J. Alloys Compd.* **699** 16
[30] Lennie A R, Knight K S and Henderson M B 2007 *Am. Mineral.* **92** 1165
[31] Law J M, Benner H and Kremer R K 2013 *J. Phys.: Condens. Matter* **25** 065601
[32] Zhang Y, Lin L F, Moreo A and Dagotto E 2022 *Appl. Phys. Lett.* **120** 023101
[33] Thota S, Ghosh S, R M, Joshi D C, Medwal R, Rawat R S and Seehra M S 2021 *Phys. Rev. B* **103** 064415

[34] Hatfield W E, Estes W E, Marsh W E, Pickens M W, ter Haar L W and Weller R R 1983 The Synthesis and Static Magnetic Properties of First-Row Transition-Metal Compounds with Chain Structures. In: Miller J S (ed) *Extended Linear Chain Compounds* (Boston, MA: Springer) p. 89
[35] Salazar A, Massot M, Oleaga A, Pawlak A and Schranz W 2007 *Phys. Rev. B* **75** 224428
[36] Ma S 2018 *Modern Theory Of Critical Phenomena* (Routledge) p. 55
[37] LIFSHITZ E M and PITAEVSKI L P 1980 *Statistical Physics* (Amsterdam: Elsevier) p. 284
[38] Markina M, Vasiliev A, Mueller J, Lang M, Kordonis K, Lorenz T, Isobe M and Ueda Y 2003 *J. Magn. Magn. Mater.* **258** 398
[39] Liu X, Wosnitza J, Löhneysen H v and Kremer R K 1995 *Phys. Rev. Lett.* **75** 771
[40] Zhao Z Y, Liu X G, He Z Z, Wang X M, Fan C, Ke W P, Li Q J, Chen L M, Zhao X and Sun X F 2012 *Phys. Rev. B* **85** 134412
[41] Kudo K, Ishikawa S, Noji T, Adachi T, Koike Y, Maki K, Tsuji S and Kumagai K 2001 *J. Phys. Soc. Jpn.* **70** 437
[42] Tkáč V, Tibenská K, Orendáčová A, Orendáč M, Šebek J, Sechovský V, Anders A G, Pavlík V and Feher A 2011 *Phys. Status Solidi* **248** 2834
[43] Sologubenko A V, Giannò K, Ott H R, Vietkine A and Revcolevschi A 2001 *Phys. Rev. B* **64** 054412
[44] Chen X, Kim J, Jia Q, Sullivan S E, Xu Y, Jarvis K, Zhou J and Shi L 2020 *Adv. Funct. Mater.* **30** 2001637
[45] Sato M, Kawamata T, Naruse K, Kudo K, Kobayashi N and Koike Y 2012 *J. Phys. Conf. Ser.* **400** 032079
[46] Kudo K, Yamazaki M, Kawamata T, Noji T, Koike Y, Nishizaki T, Kobayashi N and Tanaka H 2004 *J. Phys. Soc. Jpn.* **73** 2358
[47] Kageyama H, Suzuki H, Nohara M, Onizuka K, Takagi H and Ueda Y 2000 *Physica B* **281** 667